Generation and Rotation of 3-D Finite Element Mesh for Skewed Rotor Induction Motors Using Extrusion Technique

S. L. Ho W. N. Fu *H. C. Wong
Department of Electrical Engineering *Industrial Centre
The Hong Kong Polytechnic University, Kowloon, Hong Kong

Abstract – **A simple method to generate and rotate 3-D finite element meshes for skewed rotor induction motors using extrusion techniques is presented. Special techniques to consider the geometrical structure of skewed rotor bars are described. With the proposed method, a change in the topology of the meshes at different rotor positions needs minor modifications only. The 3-D mesh for the rotor can thus be rotated with minimal extra computing time. Here the 2-D multi-slice mesh is used as the base-planes for extruding the 3-D mesh and the results of the 2-D multi-slice model can thus be used in the 3-D model. The techniques reported in this paper greatly simplifies the 3-D mesh generation, resulting in a considerable reduction in the computing time of the associated 3-D time stepping model. The generated meshes have been used successfully in constructing the 3-D time stepping finite element model for studying the electromagnetic field of induction motors.**

Index terms – **Mesh generation, induction motors, finite element methods.**

I. INTRODUCTION

Methods for modeling the operation of electrical machines in order to estimate their performance precisely are developing quickly. For non-skewed rotor induction motors, a time stepping two dimensional (2-D) finite element method (FEM) has been developed [1]. With such approach one could use the moving-mesh technique whilst coupling the external circuit equations and mechanical equation to the field equations. Machine rotation and the non-sinusoidal quantities in the mathematical models can be taken into account in modeling the skin effect [1]. For motors with skewed rotor bars, a 2-D multi-slice model is used and the field solutions in the different slices can be solved in parallel [2]. However, in a 2-D multi-slice model the inter-bar currents in the rotors are neglected. Also the influences of the end fields are not taken into account fully. With the advent of computer technology, it is certain that the future developments in FEM modeling will move from 2-D to 3-D since a real machine is inherently 3-D in nature.

Even though many successful methods to generate a 2-D FEM mesh have been put forward, the generation of 3-D FEM mesh remains a major obstacle for machine designers wanting to use 3-D modeling [3]. In computing the electromagnetic field of induction motors using time stepping FEM, it is also essential to rotate the rotor mesh in accordance with rotor movement. The complications in the generation and rotation of 3-D FEM mesh are indeed undermining the acceptability of 3-D time stepping FEM widely in industry. Noting the 2-D techniques for such mesh rotation can now be realized easily [3], it would be a tremendous help if the 3-D mesh can be easily extruded from a 2-D mesh. Nevertheless, the geometrical structures of the skewed rotor bars in induction motors are making it difficult to apply extrusion methods directly.

The authors have developed a method to generate a 2-D multi-slice mesh of skewed rotor induction motors from the basic 2-D mesh [2]. In this paper a method to generate the 3-D mesh using an extrusion technique is described. The 2-D multi-slice meshes will be used as base-planes to generate the 3-D mesh. By introducing the concept of classifying the 'types of sides' in a triangular element, the extrusion work becomes easier, even in motors with skewed rotor bars. With the proposed algorithm the 3-D mesh has the same node distribution as the 2-D multi-slice meshes. Hence one can use the computed results of the 2-D multi-slice FEM model in the 3-D model to result in a considerable reduction in the solution time of the latter [4]. The rotor part of the 3-D mesh can also be rotated readily with minimal additional CPU time. A method to create the address vectors for indicating the storage of the sparse coefficient matrix of FEM equations is also presented. With the proposed method the computing time to re-build the address vectors as the rotor rotates at each time step is greatly reduced. The generated 3-D mesh has been used to compute the electromagnetic field of an 11 kW skewed rotor induction motor successfully [4-5].

II. GENERATION OF 2-D MULTI-SLICE MESHES

The flow chart to extrude a 3-D mesh from its 2-D multi-slice counterpart is shown in Fig. 1. Prior to the generation of the 3-D mesh, the 2-D multi-slice meshes are however constructed according to the following steps:

A. Generation of the Basic 2-D Meshes

The basic 2-D mesh at the cross-section of the induction motor are firstly generated as the base-plane for the 2-D multi-slice meshes. In order to facilitate the rotation of the 2-D rotor mesh and its subsequent 3-D counterpart, the stator mesh and rotor mesh are generated separately. The stator and rotor mesh interface in the air-gap is divided equally and the incremental angles of the rotor are set to the same value in

Manuscript received June 1, 1998.

S. L. Ho, (852) 27666170, fax 23301544, eeslho@inet.polyu.edu.hk, http://158.132.71.85/ W. N. Fu, (852) 2766 6135, eewnfu@polyu.edu.hk, http: //158.132.71.85.

The authors are grateful for the funding from the Hong Kong Polytechnic University to support this research project.

0018-9464/99$10.00 © 1999 IEEE

each time step when simulating steady-state operation. This technique will cater for motors with and without skewed rotor bars when extruding the 3-D mesh. In other words, the 2-D mesh is divided into the stator part and the rotor part, with each part including a portion of the air-gap with the proposed algorithm. For example, the air-gap in Fig. 2 is divided into three layers. Two upper layers belong to the stator and the one lower layer belongs to the rotor. For each part, the mesh is automatically generated fully using the deduction of points algorithm and the mesh refinement method [6].

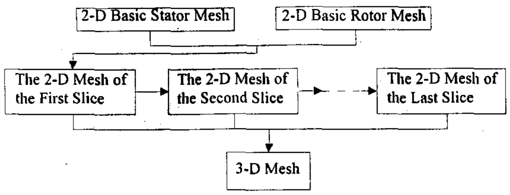

Fig. 1 The flow diagram of the 3-D mesh

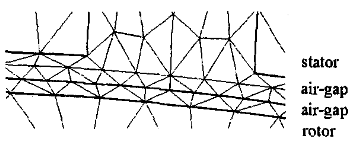

Fig. 2 The mesh in the air gap

B. Generation of the Meshes at Other Slices

The geometrical difference between the basic slice and the other slices is that the other slices have rotated progressively by a small angle due to skewing in the rotor bars. The meshes at the other slices can be easily obtained by rotating the basic rotor mesh by an appropriate small angle.

C. Connection of Slices

The nodes, elements, etc. in the FEM model are re-numbered slice by slice continually. Howerer, the data structure is essentially 2-D [2].

The time stepping FEM of the 2-D multi-slice model is very similar to that for the general 2-D model except the relationship between the adjacent slices that have been introduced in the multi-slice technique [2]. Because the solution of the 2-D multi-slice model is an approximate solution of the 3-D model and it can be obtained with less computing time, the authors have found that the 2-D results can be used profitably to reduce the solution time of its corresponding 3-D model [4].

III. Generation of 3-D Mesh

A. Extrusion of the Mesh

The 3-D mesh is generated from its 2-D multi-slice mesh using the extrusion method. Tetrahedral elements are used in the mesh discretization. Here the extrusion of one triangular element in the axial direction will generate one triangular prism which will be further divided into 3 tetrahedrals. Fig. 3 shows there are essentially six methods to divide one triangular prism into three tetrahedrals.

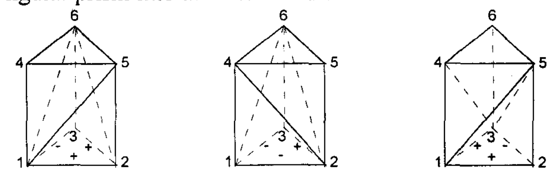

(a) Dividing method 1	(b) Dividing method 2	(c) Dividing method 3
Element 1: 1 2 3 6	Element 1: 1 2 3 6	Element 1: 1 2 3 5
Element 2: 1 2 6 5	Element 2: 1 2 6 4	Element 2: 1 5 3 4
Element 3: 1 5 6 4	Element 3: 2 6 4 5	Element 3: 3 4 5 6

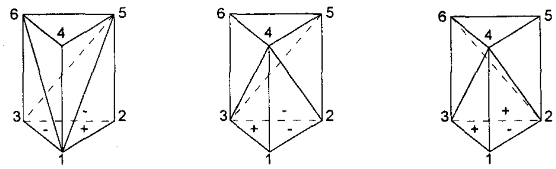

(d) Dividing method 4	(e) Dividing method 5	(f) Dividing method 6
Element 1: 1 5 2 3	Element 1: 1 2 3 4	Element 1: 1 2 3 4
Element 2: 1 5 3 6	Element 2: 2 3 4 5	Element 2: 2 3 4 6
Element 3: 1 5 6 4	Element 3: 3 4 5 6	Element 3: 2 6 4 5

Fig. 3 Six methods to divide one triangular prism into three tetrahedrals

Without losing generality, a side with nodes 1 and 2 (side 1-2) in a triangular element with nodes 1, 2 and 3 as shown in Fig. 3(a) is used as the example to introduce the concept of classifying 'types of the sides'. From the side 1-2 a surface can be extruded and this surface can be further divided into two triangles. If the dividing method of the surface is as given in Fig.4 (a), the type of side 1-2 is defined as '+'; if the dividing method of the surface is as shown in Fig. 4 (b), the type of side 1-2 is defined as '–'. According to the types of sides 1-2, 2-3 and 3-1 of the element 1-2-3, the six dividing methods of one triangular prism can be summarized as in Fig. 3 and in Table I.

(a) The sign of side is defined as '+' (b) The sign of side is defined as '–'

Fig. 4 Definition of the sign of side 1-2

To ensure the dividing methods of the common surfaces of adjacent triangular prisms are consistent, in the other words, to ensure the surface elements of the adjacent elements have the same shapes, the type of the side 1-2 of the adjacent element must be assigned as '–' if the type of the side 1-2 of the element itself is chosen as '+'; conversely, the type of the side 1-2 of the adjacent element must be assigned as '+' if the type of the side 1-2 of the element itself is '–'.

TABLE I
THE SIGNS OF THE THREE SIDES OF THE TRIANGULAR PRISM FOR THE SIX DIVIDING METHODS AS SHOWN IN FIG. 3

	Type of 1-2	Type of 2-3	Type of 3-1
Dividing method 1	+	+	–
Dividing method 2	–	+	–
Dividing method 3	+	–	+
Dividing method 4	+	–	–
Dividing method 5	–	–	+
Dividing method 6	–	+	+

Therefore, one must determine the type of the three sides of each triangle before extruding the 3-D tetrahedrals in the axial direction. The principles of this determination are:

1. In each triangle, the signs of the three sides must not be all '+' or '-' (refer to Table I).

2. The signs of the common side of adjacent triangles (including the common sides in which their relationship are determined by the periodic conditions although they are not at the same geometrical position) must be opposite. When the rotor bars are skewed, there will be an exception on the interface of the stator mesh and the rotor mesh (see Sub-heading B of this Section).

3. As the rotor mesh has to rotate, the sign of the sides at the stator interface should all be '+' or '–' while the sign of the sides at the rotor interface must be exactly opposite (only applicable to motors with unskewed rotor bars).

The signs of the three sides of each triangle can be automatically determined iteratively by comparison and adjustment. After determining the dividing methods of each triangle, it is very easy to extrude the 3-D tetrahedral meshes in the axial direction from its 2-D triangular meshes according to Fig. 3.

B. Motors with Skewed Rotor Bars

A triangular prism is to be extruded from a 2-D triangular element in the 2-D multi-slice mesh. Here the top of the prism comes from one of the slices of a 2-D multi-slice mesh, while the bottom of the same prism comes from the adjacent slice of the 2-D multi-slice mesh. When the rotor bars are skewed, the triangular prisms in the rotor part will also be skewed by a small angle. In order to ensure the surface elements on the interface of the stator mesh and the rotor mesh will have the same shapes after the rotor bars are skewed, one should divide the interface of the stator and rotor evenly. The triangular prisms of the rotor mesh on the interface should also be divided in the opposite way of the stator mesh as shown in Fig. 5. Therefore, the signs of the sides on the interface of both the stator and rotor should all be either '+' or '–'. For example, in Fig. 5, the signs of all the sides on the interface are '+'. It can be seen that the element in grey in Fig. 5 will have the same shape after the rotor bars are skewed.

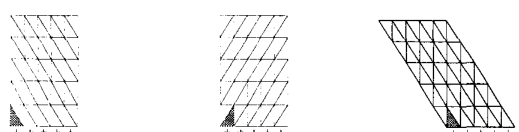

(a) Stator meshes on the interface (b) Rotor meshes on the interface before the bars are skewed (c) Rotor meshes on the interface after the bars are skewed

Fig. 5 The meshes on the interface of the stator and the rotor (noting that the stator is above the rotor)

C. Consideration of the End Windings

Because the shape of the stator end windings will not greatly affect the distribution of magnetic field and current densities in the main regions of the motor, and since both the stator current densities and the exciting sources of the field are determined from the 2-D multi-slice model in advance [4], the building of the 3-D FEM mesh for the stator windings are considerably simplified. The shapes of the cross-sections of the stator end windings are regarded as the same of that of the main stator windings. The conductors of the same stator phase under the same pole pitch are approximately connected with circle rings (refer to Fig. 9(a)). The material properties of each 3-D element are determined according to the actual material distribution of the motor and hence the stator end windings and the rotor end rings can be approximately shaped.

VI. Rotation of the Meshes

A. To Rotate the Rotor Part of the Mesh

Because the interface of the stator mesh and the rotor mesh in the air-gap is divided equally, the rotor mesh can be moved with that the minimum step length which is equal to the length of the sides on the interface. When the rotor mesh needs to be rotated with arbitrary angles, a 'shifting technique' which has been reported by the authors in [7] should be added. In order to keep the meshes in good quality, the principle of shifting the nodes on the interface is to move the nodes on the interface by as little as possible and then the nodes at the stator and rotor are moved simultaneously until they overlap. The unknowns at the inner-most nodes of the stator mesh and at the outer-most nodes of the rotor mesh are connected by virtue of the 'periodic boundary conditions'. That is to say, when the rotor rotates, the shape of the rotor mesh will not be changed, but the coordinates and the periodic boundary conditions will. Thus the stator mesh and the rotor mesh are generated once and once only. Because the meshes can be kept unchanged, the 'noise' caused by the changes in the meshes can be eliminated [8].

Both the 2-D multi-slice meshes and the 3-D mesh use this method to rotate the rotor meshes.

B. To Generate the Address Vectors of Sparse Matrix

The sparse coefficient matrixes of 2-D FEM equations and 3-D FEM equations are stored in a compressed style because these equations will be solved using the ICCG method. Zero elements will not be stored. The address vectors are only needed to indicate where the elements in the matrix are not zero. To establish such address vectors one needs to make a search to find the neighboring nodes of each node. For a 3-D mesh such search needs a lot of computing time.

On the other hand, since the stator mesh and the rotor mesh are generated separately, one can store the topology of the stator mesh and the rotor mesh in a data file. The whole mesh which connects the stator mesh and the rotor mesh together includes only the boundary conditions on the interface into its topology. When the rotor rotates, only minor modification to the nodes on the interface is needed in order to establish the topology of the whole mesh. Thus with the exception of the first step, the time to do the search will be greatly reduced in the subsequent steps.

V. EXAMPLE

The method as described has been used to generate the 3-D mesh of an 11 kW skewed rotor induction motor (4 poles, 48 stator slots and 44 rotor slots) which is modeled by using a 3-D time stepping FEM. The solution domain includes the iron frame in the outer-most surface of the periphery, the shaft in the inner-most surface of the periphery and the endshields in the axial direction. The shaft is simplified as a hollow cylinder so that the number of nodes can be reduced slightly while the accuracy of the model will not be affected. Because the rotor bars are skewed, the total axial length of the machine in the axial direction should be included. In the cross-sectional direction, only one pole pitch in the solution domain is required.

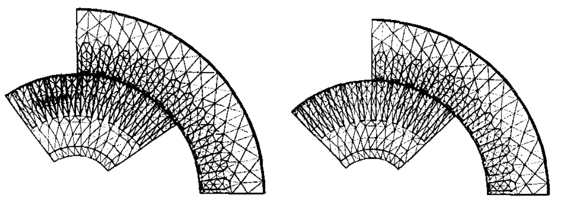

(a) At the first slice of the iron core (b) At the eighth slice of the iron core

Fig. 6 FEM meshes of an 11 kW skewed motor after a rotation of 34° (each slice has 952 nodes, 1703 elements)

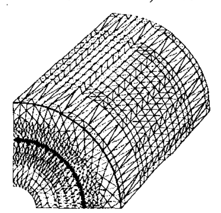

Fig. 7 An outer surface view of a 3-D FEM mesh of an 11 kW induction motor (with 15232 nodes and 76635 elements)

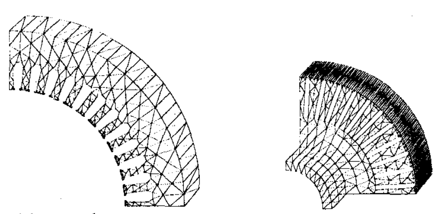

(a) stator iron core (b) rotor iron

Fig. 8 A 3-D FEM mesh of the iron cores (Only one piece of iron core is shown)

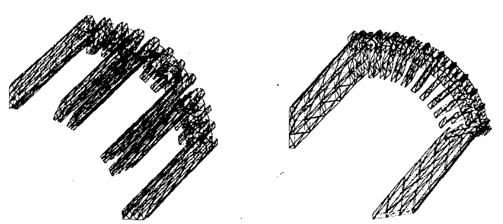

(a) stator windings (b) rotor bars and end ring

Fig. 9 3-D FEM mesh of the windings (Half of the windings are shown. Only two conductors in each stator phase are shown. Also only two bars in the rotor cage are shown.)

Two of the multi-slice meshes are shown in Fig. 6. An outer surface of the developed 3-D mesh is shown in Fig. 7. The meshes of the stator iron core, rotor iron core, stator windings, rotor bars and rotor end ring are shown in Fig. 8 and Fig. 9.

By using the method to store the topology of the stator and rotor meshes in a data file, the authors have found that the CPU time required to generate the address vectors of the sparse coefficient matrix can be reduced from 33.3 min. to 0.88 min. on a Pentium / 166 MHz personal computer for each time stepping (except the initial time step).

The developed 3-D time stepping FEM coupled with a 2-D multi-slice time stepping FEM have been used successfully to estimate the stray losses of skewed rotor induction motors. The results have been reported in [4].

IV. CONCLUSION

A 3-D FEM mesh of skewed rotor induction motors can be easily extruded from its 2-D multi-slice mesh. The mesh generation method is simple, robust, and the rotor mesh can be rotated easily. The topology of the meshes needs minor modification at different rotor positions and the mesh can be rotated with minimal additional CPU time. Because of the close relationship between the 3-D mesh and the 2-D multi-slice meshes, the results of the 2-D multi-slice model can be used in the corresponding 3-D model. A substantial reduction in the computing time of 3-D FEM studies can thus be obtained.

REFERENCES

[1] S. Williamson, "Induction Motor Modelling Using Finite Elements," *Proc. of Inter. Conf. on Electrical Machines*, Paris, France, 5-8 September, 1994, pp.1-8.

[2] S. L. Ho and W. N. Fu, "A Comprehensive Approach to the Solution of Direct-Coupled Multislice Model of Skewed Induction Motors Using Time Stepping Eddy-Current Finite Element Method", *IEEE Trans. Magn.* Vol.33, No.3, May, 1997, pp.2265-2273.

[3] P. L. George, "Automatic Mesh Generation-Application to Finite Element Methods", *John Wiley & Sons Ltd*, England, 1991.

[4] S. L. Ho, W. N. Fu and H. C. Wong, "Estimation of Stray Losses of Skewed Induction Motors Using Coupled 2-D and 3-D Time Stepping Finite Element Methods", *IEEE Trans. Magn.*, Vol.34, No.5, September, 1998, pp. 3102-3105.

[5] S. L. Ho and W. N. Fu, "Solution of A 3-D Complex Finite Element Model of Skewed Rotor Induction Motors Using An Iterative Method", *The 1997 IEEE International Electric Machines and Drives Conference*, Milwaukee, Wisconsin, May 18-21, 1997 (Accepted by *IEEE Trans. on Energy Conversion.*)

[6] S. L. Ho and W. N. Fu, "A Fully Automatic Mesh Generation Method for the Movement Field Modelling", The Second Chinese International Conference on Electrical Machines, Hangzhou, China, 31 August - 2 September 1995, pp.624-630.

[7] S.L.Ho, W.N.Fu, H.C.Wong and C.Y.Hung, "A Time Stepping FEM Model of Induction Motors Running on Personal Computers", *Fifth International Conference on Modelling and Simulation of Electric Machines, Converters and Systems*, Sept. 17-19, 1996, Saint, Nazaire, France, pp.461-466.

[8] I.Tsukerman, "Accurate Computation of 'Ripple Solutions' on Moving Finite Element Meshes", *IEEE Trans. Magn.*, vol. 31, no. 3, pp. 1472-1475, May 1995.